

# Possible mechanism of protective effect of melatonin against carbendazim-induced hepatotoxicity in mature male rats: histological, immunofluorescence, and biochemical evaluations

Ali Menatnia<sup>1</sup>, Ali Louei Monfared<sup>1\*</sup>, Hassaneen Sharoot<sup>2</sup>

<sup>1</sup> Department of Histology, Faculty of Veterinary Sciences, Ilam University, Ilam, Iran; <sup>2</sup> Department of Anatomy and Histology, College of Veterinary Medicine, University of Al-Qadisiyah, Al-Qadisiyah, Iraq.

Article Info	Abstract
<b>Article history:</b> Received: 13 September 2024 Accepted: 05 November 2024 Available online: 15 August 2025	<p>This study investigated carbendazim (CBZ)-induced hepatic dysfunction and the mechanistic pathway regarding the protective effect of melatonin (MEL). Twenty-eight male rats were grouped as follows: Control, CBZ (150 mg kg<sup>-1</sup>), MEL (20.00 mg kg<sup>-1</sup>), and CBZ + MEL. The experiment was conducted for 60 days. Tissue samples were stained with Hematoxylin and Eosin and immunofluorescence methods to examine apoptotic pathway. Also, hepatic enzymes and miR-122 expression were evaluated. The findings indicated that the CBZ group exhibited an increase in degenerated hepatocytes, hyperemia of sinusoids, and leukocyte infiltration, accompanied by elevated levels of aspartate aminotransferase and alanine aminotransferase, as well as up-regulation of miR-122. Also, there was a significant increase in the fluorescence intensities of caspase-3 and Bax in the CBZ group, whereas a substantial reduction in the fluorescence intensity of Bcl-2 was recorded. In contrast, the simultaneous administration of MEL alongside CBZ was shown to be effective in improving histological structure, decreasing levels of aspartate aminotransferase and alanine aminotransferase, reducing the apoptosis index, and modulating the expression of miR-122 in comparison with the CBZ-only group. The increased expression of miR-122 noted in the CBZ group may correlate with an elevation in the immunoreactivity of apoptosis markers and alterations in liver architecture. Additionally, MEL seems to alleviate CBZ-induced hepatotoxicity by down-regulating miR-122 expression, diminishing the fluorescence intensity of caspase-3 and Bax, and enhancing the immunoreactivity of Bcl-2. Collectively, the regulation of miR-122 may serve as a potential mechanism by which MEL confers its protective effects against liver damage induced by CBZ.</p>
<b>Keywords:</b> Carbendazim Histology Liver Melatonin Rat	

© 2025 Urmia University. All rights reserved.

## Introduction

Liver damages are among the serious challenges for human health around the world. Various factors, such as chemical pollutants, drugs, and alcohol, can cause liver injury.<sup>1</sup> Nevertheless, despite all the studies done so far, there are very few suitable therapeutic compounds for liver injuries and diseases.<sup>2</sup> On the other hand, there is a growing concern that some agricultural agents, such as carbendazim (CBZ), adversely affect the structure and function of the liver. As a systemic fungicide, CBZ is commonly used in agriculture and has wide applications for controlling fungal diseases in forestry and veterinary medicine. The CBZ is also employed to protect the facade of buildings against fungi. Besides, CBZ contamination in superficial waters mainly results from the discharge of

treated domestic sewage.<sup>3</sup> The inhalation of fungicide or consumption of contaminated water, agricultural raw material, and frozen vegetables are the main routes of human or animal exposure to CBZ.<sup>4</sup> It has also been reported that CBZ causes liver damage in mice and zebrafish.<sup>5</sup> Numerous experimental studies have demonstrated that CBZ adversely affects hepatic integrity, which can be related with the induction of apoptosis, oxidative stress, and inflammation.<sup>6-9</sup> Based on past research, CYP<sub>1A2</sub> has been identified as the main enzyme responsible for the hepatic metabolic activation of CBZ. Also, increasing the administered CBZ concentration not only causes cytotoxicity but also changes the affinity of structural proteins in hepatocytes, suggesting a link between hepatotoxicity and the metabolic activation of CBZ.<sup>5</sup>

### \*Correspondence:

Ali Louei Monfared. DVM, PhD  
Department of Histology, Faculty of Veterinary Sciences, Ilam University, Ilam, Iran  
E-mail: a.loueimolfared@ilam.ac.ir



This work is licensed under a Creative Commons Attribution-NonCommercial-ShareAlike 4.0 International (CC BY-NC-SA 4.0) which allows users to read, copy, distribute and make derivative works for non-commercial purposes from the material, as long as the author of the original work is cited properly.

Several researchers have efforts to find a novel protective agent to reduce the liver adverse effects of CBZ. For example, in one study, rats co-treated with quercetin and CBZ demonstrated marked improvement in both physiological and structural alterations of liver compared to the CBZ-alone ones.<sup>9</sup> Also, in another work, due to its genoprotective and free radical scavenging activities, *Nigella sativa* oil was associated with normalized hepatic structural architecture, and minimized the elevated liver enzymes in a rat model of CBZ-induced hepatic damage.<sup>8</sup> Furthermore, the possible protective effects of administration of olive leaves extract on CBZ-induced hepatic, renal, and testicular injuries have been investigated previously.<sup>6</sup> Salihu *et al.*, have investigated the protective effects of active fraction of ginger on the liver and kidney alterations in rats exposed to CBZ. Their examinations not only revealed renal and hepatic dysfunction due to the CBZ but also certificated the protective characteristic of active ginger ingredients against CBZ toxicity.<sup>7</sup>

Melatonin (MEL; N-acetyl-5-methoxy-tryptamine) is an indolamine hormone mainly synthesized from the amino acid tryptophan by the pineal gland and many other organs in mammals. This lipophilic and polymorphic hormone plays an important role in eliminating free radicals and stimulating anti-oxidant enzymes and thus, protecting various tissues, including the liver, against different toxicants.<sup>10</sup> Also, it has been shown that MEL is essential for healthy metabolism of proteins and fats by acting as a synchronizer of circadian rhythm, seasonal reproduction, and also anti-oxidant effects.<sup>11</sup> Finally, MEL has been reported to prevent oxidative stress and cytotoxicity caused by cadmium through local signal transducer and activating of transcription-3 pathway, consequently improving mitochondrial function during stress caused by cadmium.<sup>12</sup>

A review of previous studies showed that MEL improves liver and pancreatic tissues injuries in streptozotocin-diabetic rats *via* different anti-oxidant effects.<sup>10</sup> Also, the protective effect of MEL against herbicides-induced hepatotoxicity in rats has been proven in another investigation.<sup>13</sup> Furthermore, the potential protective anti-oxidant role of MEL in cyclosporine - induced hepatotoxicity was examined in Sprague-Dawley rats. It has been concluded that MEL may assist to protect against cyclosporine -induced damage to liver tissues possibly through effects on the anti-oxidant system.<sup>14</sup> Nevertheless, there is not much research regarding the possible effect of MEL on the histological changes of the liver caused by CBZ in rats. Therefore, the aim of the current research was to investigate the possible mechanism and the effect of MEL on the histological structure of the liver of rats treated with CBZ. From the results of this research, the possible effects of the MEL against CBZ toxicity may be commented.

## Materials and Methods

**Chemicals.** Carbendazim (purity: 97.00%) and melatonin (powder,  $\geq 98.00\%$ ) were purchased from Sigma-Aldrich Chemicals Company (St. Louis, USA). All other chemicals were obtained from Merck Company (Darmstadt, Germany), unless otherwise stated.

**Animals.** This study followed the institutional guidelines regarding the care and use of laboratory animals. The study protocol was approved by the Animal Experiment Committee in Ilam University, Ilam, Iran (No: IR.ILAM.REC.1402.015). All animals were bred and handled in accordance with the guidelines for the care and use of laboratory animals. Twenty-eight male Wistar rats (7 - 9 weeks old and 220 - 250 g) were raised in a 12 hr light/dark cycle at constant room temperature ( $22.00 \pm 2.00$  °C) with a standard diet in the Veterinary Medicine Laboratory Animal Husbandry Center, Ilam, Iran.

**Study protocol.** After adaptation to new laboratory conditions, the animals were randomly grouped ( $n = 7$ ) as follows: Negative control group: Rats were intra-peritoneally injected with physiological saline, CBZ group: Rats were given  $150 \text{ mg kg}^{-1}$  CBZ by daily oral gavage method, CBZ + MEL group: Rats were received  $150 \text{ mg kg}^{-1}$  CBZ by gavage method and simultaneously injected with MEL at a dose of  $20.00 \text{ mg kg}^{-1}$ , and MEL group: Rats were intra-peritoneally injected with  $20.00 \text{ mg kg}^{-1}$  MEL one time. The CBZ and MEL doses were based on previously published research.<sup>15-18</sup> The experiment lasted 60 days. At the end of the treatments, the animals were anaesthetized using intra-muscular injection of  $50.00 \text{ mg/ kg-1}$  body weight ketamine hydrochloride and  $5.00 \text{ mg/ kg-1}$  xylazine hydrochloride. Then, blood samples were collected and serum was separated. Serum levels of alanine aminotransferase (ALT) and aspartate aminotransferase (AST) were then assessed using an automatic analyzer (BT-1500 Biotecnica Instruments, Roma, Italy) and commercial assay kits (ALT: Biorexfars, Shiraz, Iran), and International Federation of Clinical Chemistry and Laboratory Medicine method without pyridoxal phosphate; AST: Biorex Fars).

**Histology and histomorphometry.** Excised livers samples were fixed in a 10.00% buffered formalin solution for 48 hr. They were subjected to standard routine tissue processing technique, including dehydration by graded ethyl alcohol concentrations, clearing in xylene, and embedding in paraffin. Then,  $5.00\text{-}\mu\text{m}$ -thick tissue sections were stained with Hematoxylin and Eosin method. Histological photographs of liver were taken using a light microscope (BH-2; Olympus, Tokyo, Japan) equipped with a digital camera and image analysis software (True Chrom Metrics; Tucsen, Fuzhou, China). Afterwards, all sections were evaluated for the degree of liver alterations, and

photographs were evaluated quantitatively. For histomorphometry examination, six random fields of each section were selected and in each of them, the following parameters were counted and expressed numerically between 0 and 100% according to the methods proposed previously.<sup>19,20</sup> The percentage of normal and dilated veins, the percentage of normal or necrotic hepatocytes, and the rate of infiltrating inflammatory cells *per mm*<sup>2</sup> of histological cross-sections.

**Immunofluorescence examinations.** Sections were subjected to dehydration and rehydration with xylene and graded alcohol, respectively. To detect non-specific tissue antigens, the slices were placed in citrate buffer for 10 min in an autoclave (pH: 7.40, 121 °C, and two atmospheres). The activity of endogenous peroxidase was removed by 3.00% H<sub>2</sub>O<sub>2</sub> solution for 15 min. Dako blocking reagent was used to remove non-specific connections of antibody with tissue antigens. Sections were then incubated with the primary antibody against BAX, Bcl-2 and, caspase-3 (1/400) overnight at 4.00 °C. After washing in phosphate-buffered saline, goat anti-rabbit immunoglobulin G (H+L, fluorescein isothiocyanate conjugated, and diluted 1/10,000 in blocking solution) was added to the sections for 1 hr at room temperature. After three times washing in phosphate-buffered saline, 1.00 µg mL<sup>-1</sup> 4',6-diamidino-2-phenylindole was added to the specimens (30 min at room temperature and dark medium) for cell nuclei staining. The sections were observed under fluorescence microscope (BX50; Olympus) and photographed at 200× magnification with an Olympus DP72 camera. The nuclear morphology and distribution of apoptosis-related proteins in the hepatic tissue were estimated by densitometry technique and analyses of cells with ImageJ Software (National Institutes of Health, Bethesda, USA).

**Quantitative real-time reverse transcription polymerase chain reaction (qRT-PCR) assay.** For qRT-PCR assay, 100 mg of liver tissue was separated and placed in a test tube with 1.00 mL radioimmunoprecipitation assay buffer (pH: 8.00; sodium chloride: 150 mM, sodium dodecyl sulfate: 0.10%, Tris: 25.00 mM, phenylmethylsulfonyl fluoride: 1.00 mM, and sodium fluoride: 50.00 mM). It was mixed and homogenized using a homogenizer. In order to determine the amount of protein in the samples, the Bradford method was used.<sup>21</sup> To investigate the expression level of miR-122 in liver tissue by qRT-PCR, total RNA was extracted from 50.00 mg of each liver sample using the miRcute Isolation Kit (Tiangen, Beijing, China), following the supplier's protocol. The purity of RNA was determined by measuring the optical density at the ratio of 260/280 using a dedicated micro-volume measurement cuvette Eppendorf µCuvette® G1.0 (Eppendorf, Hamburg, Germany). Purified RNA from each sample, containing 300 ng of total RNA, was rapidly reverse transcribed into first-strand cDNA using the

miRNA miRcute First-Strand cDNA Synthesis Kit (Tiangen). Subsequently, qRT-PCR was performed using the Applied Biosystems StepOnePlus™ Real-Time PCR System (Thermo Fisher Scientific, Foster City, USA) by miRcute miRNA qPCR Detection Kit, SYBR Green (Tiangen), and a specific primer for miR-122. The primers used were as follows: miR-122-Rat-Forward: GGAGTGTGACAATGGT GTTTG, cDNA Adapter Reverse: GAACATGTCTGCGTATCTC, U<sub>6</sub>-Forward: TGCTTCGGCA GCACATATAC, and U<sub>6</sub>-Reverse: AGGGGCCATGCTAATC TTCT. The reaction was performed under the following conditions: 94.00 °C for two min, 94.00 °C for 20 sec, and 60.00 °C for 34 sec. The relative amount of miR-122 tested for each sample was normalized to the level of U<sub>6</sub> as an endogenous control gene.

**Statistical analysis.** The results were analyzed using SPSS Software (version 16.0; SPSS, Inc., Chicago, USA). The descriptive values were expressed as the mean ± standard error. To evaluate the normality of the data, the Kolmogorov Smirnov test was used. To determine the difference between the groups, one-way analysis of variance, followed by Tukey *post hoc* tests for multiple comparisons was exploited. A *p*-value less than 0.05 was considered statistically significant.

## Results

During this study, one death occurred in the group treated with CBZ. Nevertheless, the animals did not show clinical symptoms during the study. Macroscopic observations showed that animals did not have any anatomical abnormalities. To test whether MEL has hepatoprotective activities, the biochemical and histological changes were evaluated after a liver damage had been induced by CBZ.

To evaluate liver injury, liver function enzymes (AST and ALT) in sera were evaluated. The CBZ administration significantly (*p* < 0.05) increased the measured liver function indices in comparison with the control group. Meanwhile, treatment of rats with MEL + CBZ caused marked decrease (*p* < 0.05) in AST and ALT levels in comparison with the CBZ group (Fig. 1).

The results confirmed obvious hepatic tissue alterations, including increase in degenerated hepatocytes, hyperemia of sinusoids, and leukocyte infiltration, after CBZ treatment. Interestingly, MEL had a protective effect on the liver parenchyma and general integrity of the hepatic blood vessels. Only slight blood congestion was seen in some sections (Figs. 2 and 3). As illustrated in Figure 3, the hepatic tissues of CBZ-treated rats manifested a significant decline in the numbers of normal hepatocytes and a considerable rise in the numbers of necrotic hepatocytes, as well as significantly increased leukocyte infiltration in the periportal and centro-lobular zones (Fig. 4).

On the contrary, CBZ + MEL group showed a significant decrease in the scoring of almost all lesions compared to the group receiving CBZ, and in some parameters it was almost similar to the control group (Fig. 4).

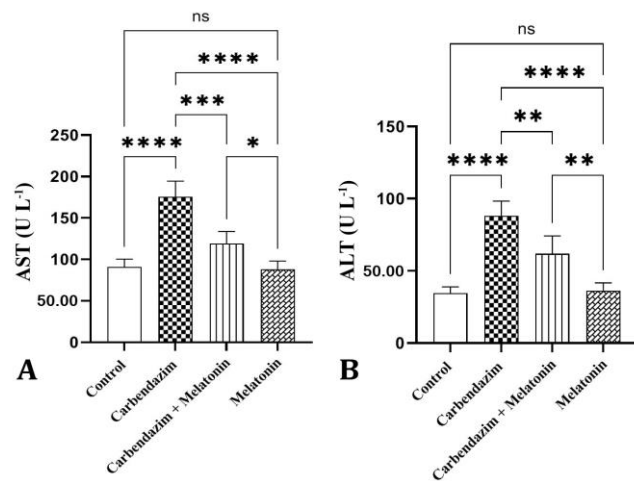


**Fig. 1.** The effect of melatonin on changes in serum liver function markers caused by carbendazim in rats. **A)** Aspartate amino-transferase (AST) level in serum; **B)** Alanine aminotransferase (ALT) level in serum. At the top of each column, \* means a significant difference at the  $p < 0.05$  level, \*\* means a significant difference at the  $p < 0.01$  level, \*\*\* means a significant difference at the  $p < 0.001$  level, and \*\*\*\* means a significant difference at the  $p < 0.0001$  level. ns: non-significant.

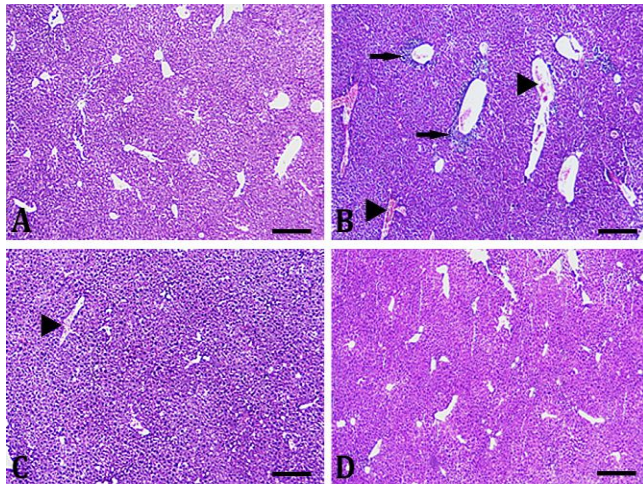


**Fig. 2.** Histological analysis of rat liver tissue treated with carbendazim (CBZ) and melatonin (MEL) alone or in combination with each other. **A)** Control group: Ordinary morphology of liver parenchyma can be seen; **B)** CBZ group: Severe hepatic tissue abnormality can be seen (black triangles indicate hyperemia and black arrows represent leukocyte infiltration); **C)** CBZ + MEL group: Significant improvement in the order and structure of liver parenchymal cells and overall structure of liver blood vessels is obvious; **D)** MEL group: The normal histo-architecture of the liver is observed, being similar to the control group (Hematoxylin and Eosin staining, Bars = 188  $\mu$ m).

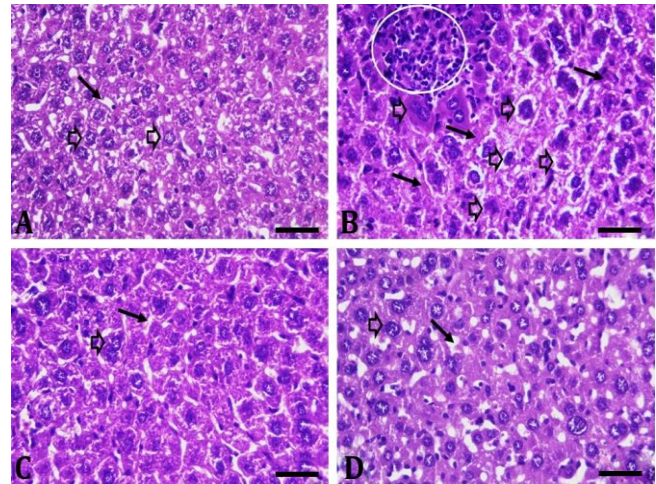


**Fig. 3.** Histological analysis of rat liver tissue treated with carbendazim (CBZ) and melatonin (MEL) alone or in combination with each other. **A)** Control group: The regular morphology of the liver parenchyma along with normal structure and size of the liver sinusoids without any hyperemia is seen; **B)** CBZ group: An increase of degenerated and vacuolated liver cells (arrows), expansion and hyperemia of sinusoids (arrows head), and infiltration of infiltrating inflammatory cells can be seen in the central lobular areas illustrated by a white circle; **C)** CBZ + MEL group: A significant improvement is observed in the cellular order, and structure of liver parenchymal cells and blood vessels. Also, infiltration of infiltrating inflammatory cells is not seen in this group; **D)** MEL group: The normal hepatic tissue architecture is observed, being similar to the control group (Hematoxylin and Eosin staining, bars = 19.00  $\mu$ m).

To investigate the protective effect of MEL on apoptosis induced by CBZ, the expressions of caspase-3 (apoptosis executive protein), Bax (pro-apoptotic factor), and Bcl-2 (anti-apoptotic factor) in liver tissue were detected by and immunofluorescence stainings. Caspase-3, Bax, and Bcl-2 immunoexpressions in hepatic tissues of all experimental groups are illustrated in Figures 5-8, respectively.

As shown in Figures 5-8, unlike the control group, the fluorescence intensity of caspase-3 and Bax in the liver tissue increased significantly, whereas the fluorescence intensity of Bcl-2 decreased significantly in the CBZ group. However, treatment of rats with MEL plus CBZ up-regulated the immunoexpression of Bcl-2 and down-regulated the immunoexpression of caspase-3 and Bax (Figs. 5-8).

The expression pattern of miR-122 in liver tissue belonging to the different experimental groups was tested by qRT-PCR method. To confirm the amplification of the specific parts of miR-122, absence of non-specific genes, and pairing of primers, the correctness of performing qRT-PCR reactions was confirmed by drawing standard efficiency graphs, amplification plots, and melting curves.

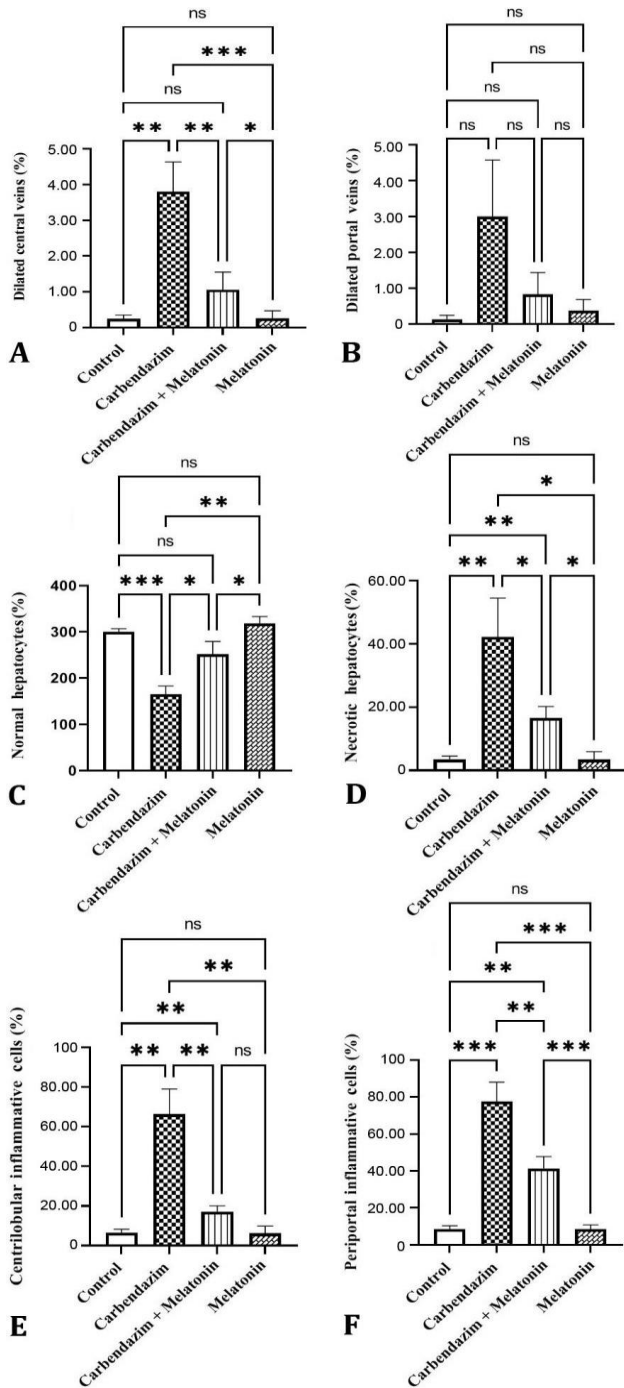


**Fig. 4.** Effect of melatonin administration on histometric parameters of liver tissue sections in animals treated with carbendazim. **A)** Percentage of dilated and hyperemic central lobular veins; **B)** Percentage of dilated and hyperemic portal veins; **C)** Percentage of normal hepatocytes; **D)** Percentage of necrotic hepatocytes; **E)** Percentage of inflammatory cells in the vessels of the center of the lobule; **F)** Percentage of inflammatory cells in the vessels around the portal area. At the top of each column, \* means a significant difference at the  $p < 0.05$  level, \*\* means a significant difference at the  $p < 0.01$  level, \*\*\* means a significant difference at the  $p < 0.001$  level, and \*\*\*\* means a significant difference at the  $p < 0.0001$  level. ns: non-significant.

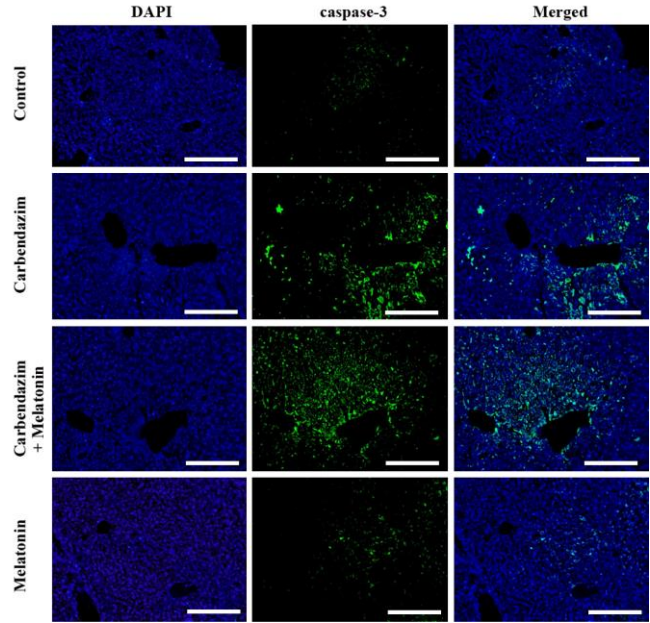


**Fig. 5.** Protective effect of melatonin on carbendazim-induced liver apoptosis in rats. Immunofluorescence staining of caspase-3 (green color) in the liver tissue. 4',6-diamidino-2-phenylindole (DAPI; blue dye) was used to stain the nuclei, (bars = 50.00  $\mu\text{m}$ ).

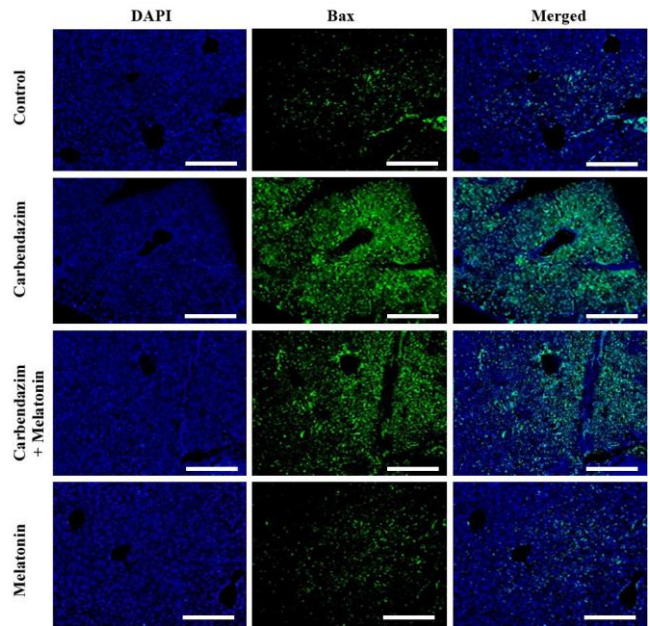


**Fig. 6.** Protective effect of melatonin on carbendazim-induced liver apoptosis in rats. Immunofluorescence staining of Bax (green color) in the liver tissue. 4',6-diamidino-2-phenylindole (DAPI; blue dye) was used to stain the nuclei, (bars = 50.00  $\mu\text{m}$ ).

As shown in Figure 8D, miR-122 was strongly expressed in liver tissue of CBZ group compared to control group. A very low expression of miR-122 was found in the liver tissue in control and MEL receiving groups. Also, a significant decrease in the expression of miR-122 was observed in CBZ + MEL group compared to CBZ group.

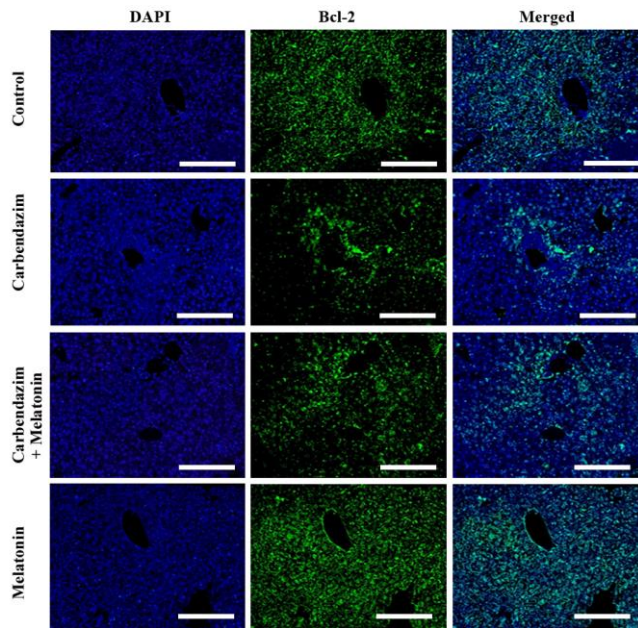


**Fig. 7.** Protective effect of melatonin on carbendazim-induced liver apoptosis in rats. Immunofluorescence staining of Bcl-2 (green color) in the liver tissue. 4',6-diamidino-2-phenylindole (DAPI; blue dye) was used to stain the nuclei, (bars = 50.00  $\mu$ m).

## Discussion

Recently, many reports have found that pesticides and fungicides cause several human and animal health problems, including liver dysfunction.<sup>4,5</sup> The MEL is a pineal gland-originated hormone that has beneficial health effects. However, there is little scientific information regarding the effect of MEL on CBZ-induced liver damage. Therefore, the present study investigated the possible mechanism of MEL effect in CBZ-induced liver damage in rats. The results of the present study showed widespread degeneration of hepatocytes with vacuolated cytoplasm, remarkable increase in the number of necrotic hepatocytes, hyperemia of the sinusoids, and centrolobular inflammation in the CBZ group. These findings suggest destructive effects of CBZ and are consistent with the results of previous study involved detrimental hepatic changes caused by CBZ.<sup>9,22-24</sup> Nevertheless, the simultaneous administration of MEL alongside CBZ caused a significant improvement in the microscopic structure of the liver, including hepatocyte recovery, decreasing of inflammation, and promotion of the liver blood vessels integrity. Also, a significant reduction in the scores of almost all lesions was seen compared to the group receiving CBZ.

Previous studies have reported that CBZ administration in rats has the ability to induce apoptosis, consequently leading to hepatic dysfunction in a dose- and time-dependent manner.<sup>22,24</sup> To investigate the protective effect of MEL on apoptosis induced by CBZ, the

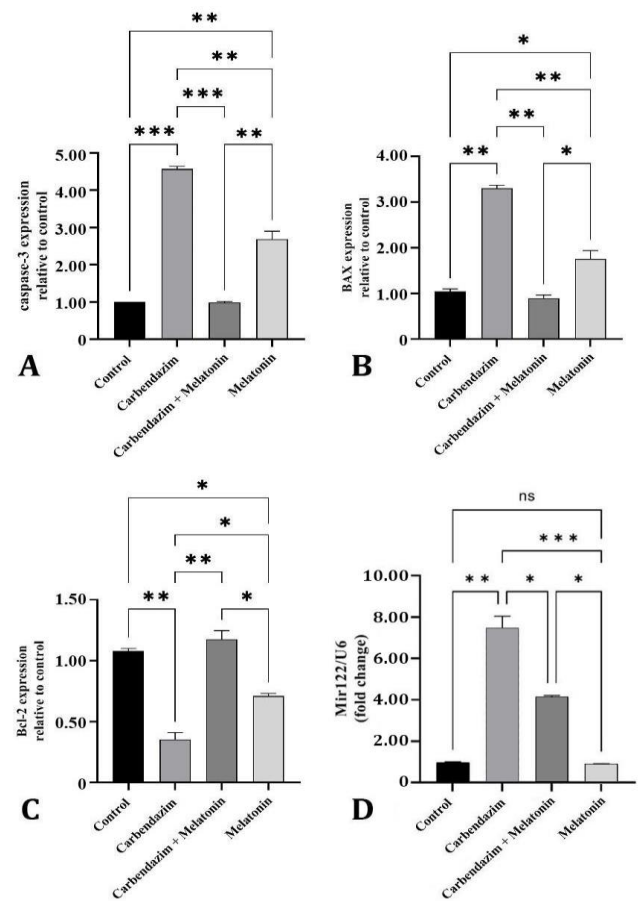


**Fig. 8.** Densitometry technique and quantitative analysis of **A)** caspase-3, **B)** Bax **C)** Bcl-2 positive areas among different groups. **D)** Comparison of miR-122 expression level in liver tissue in different experimental groups. The U<sub>6</sub> was used as an internal control. At the top of each column, \* means a significant difference at the  $p < 0.01$  level, \*\* means a significant difference at the  $p < 0.001$  level, and \*\*\* means a significant difference at the  $p < 0.0001$  level. ns: non-significant.

expressions of caspase-3 (apoptosis executive protein), Bax (pro-apoptotic factor), and Bcl-2 (anti-apoptotic factor) in the liver tissue were detected by immunohistochemical and immunofluorescence staining. Our results revealed for the first time that MEL has strong anti-apoptotic effect manifested by weak immunohistochemical staining of caspase-3 and Bax, as well as strong immunoactivity for Bcl-2 in liver sections from CBZ-treated rats. Generally, Bax, caspase-3, and Bcl-2 are the main proteins that regulate apoptosis by interacting with mitochondrial membrane permeability.<sup>25-27</sup> These findings suggest that MEL can effectively reduce CBZ-induced liver apoptosis. In accordance with the current results, a recent study showed that MEL reduced hepatocyte ferroptosis induced by lead or lipopolysaccharide exposure through activation of adenosine monophosphate-activated protein kinase phosphorylation.<sup>28</sup> Also, due to its lipophilic properties and small size, MEL can easily pass cell membrane,<sup>29-30</sup> and

prevent protein, DNA, and lipid peroxidation damages. In particular, by reducing oxidative stress in mitochondria, MEL can also normalize mitochondrial homeostasis, finally preventing apoptosis.<sup>31</sup> In addition, due to its multi-functional anti-apoptotic and anti-apoptotic regulatory effects, it has been proven that MEL is a promising compound for protecting tissues against cadmium and carbon tetrachloride induced hepatotoxicity.<sup>32-34</sup>

Along with our histological results, the biochemical findings also confirmed the hepatotoxicity of CBZ. So, the serum levels of AST and ALT, the most indicative markers of liver deterioration, showed significant elevations. These findings are in accordance with the previous studies.<sup>9,22,24</sup> Contrary to this, applying a MEL significantly reversed serum AST and ALT levels. These findings may indicate that MEL can effectively induce protection of liver function against CBZ-induced hepatotoxicity. Regarding the ameliorating effects of MEL on liver enzyme's function, similar results have been reported following exposure to cadmium.<sup>32</sup>

The MEL as a natural anti-oxidant, lipophilic, and polymorphic hormone has long been known to have many biological activities, including protective effects against liver damage.<sup>2</sup> However, little information is available about the possible mechanism of its beneficial effects on the liver in the case of CBZ hepatotoxicity. Therefore, in the present study, the hepatic expression of miR-122 as the most abundant miRNA in human liver tissue was investigated. The current results revealed marked activation of the miR-122 in the hepatic tissues of rats treated with CBZ. Previous studies have also indicated that serum levels of miR-122 increase after the induction of liver injuries.<sup>35-36</sup> On the other hands, MEL could significantly inhibit the increase of hepatic miR-122 expression. Thus, as a possible mechanism, the inhibitory effect of MEL on the miR-122 expression could be correlated with its hepatoprotective effect, being demonstrated in this research by histological, immunofluorescence, and biochemical examinations. Accordingly, a significant association between liver structural changes and the plasma concentration of miR-122 has been shown previously.<sup>35</sup>

One of the limitations of this research was the lack of electron microscopy to examine the details of the structure of the liver and the organs involved in CBZ intoxication, as well as the protective effects of MEL. Another limitation was the absence of determination of anti-inflammatory factors related to MEL-induced hepatoprotection. So far, no study has reported the protective effect of MEL against liver toxicity caused by CBZ; so, the present findings are worth innovation. One of the strengths of this research is the investigating of the possible relationship between hepatic tissue alterations, apoptosis pathway, and miR-122 expression. However, it is important to acknowledge that the discovery of the

relationship between MEL, apoptosis, and miR-122 expression requires further investigation.

In the present study, increased expression of miR-122 in CBZ group could be related to increased immunoreactivity of apoptosis marker proteins, and consequently liver histological abnormalities. Furthermore, MEL-mediated hepatoprotection in CBZ-treated rats could involve regulatory mechanisms on miR-122 silencing and anti-apoptosis pathways. Taken together, our results provide a new insight into the ameliorative role of MEL supplementation against CBZ-induced hepatotoxicity.

### Acknowledgments

We extend sincere gratitude to the Ilam University, Ilam, Iran, and University of Al-Qadisiyah, Al-Qadisiyah, Iraq, for providing laboratory facilities and technical supports. The authors would like to thank the respected research assistance of Ilam University, Ilam, Iran, for their cooperation in conducting this research. We are grateful to Dr Hamzeh Zangeneh for statistical guidance and Dr Zahra Naderi for critical review of the manuscript. The authors would like to thank Dr. Saleh Azizian, Dr. Salman Soltani, and Dr. Hajar Azizian for their great assistance during samples preparation, biochemical tests, and histopathological examinations.

### Conflict of interest

All authors declare no conflict of interest.

### References

1. Barouki R, Samson M, Blanc EB, et al. The exposome and liver disease - how environmental factors affect liver health. *J Hepatol* 2023; 79(2): 492-505.
2. Zhang JJ, Meng X, Li Y, et al. Effects of melatonin on liver injuries and diseases. *Int J Mol Sci* 2017; 18(4): 673. doi: 10.3390/ijms18040673.
3. Merel S, Benzing S, Gleiser C, et al. Occurrence and overlooked sources of the biocide carbendazim in wastewater and surface water. *Environ Pollut* 2018; 239: 512-521.
4. Stachniuk A, Szmagara A, Czczko R, et al. LC-MS/MS determination of pesticide residues in fruits and vegetables. *J Environ Sci Health B* 2017; 52(7): 446-457.
5. Shi J, Zhao M, Li K, et al. Metabolic activation and cytotoxicity of fungicide carbendazim mediated by CYP1A2. *J Agric Food Chem* 2022; 70(13): 4092-4101.
6. Zari TA, Al-Attar AM. Therapeutic effects of olive leaves extract on rats treated with a sublethal concentration of carbendazim. *Eur Rev Med Pharmacol Sci* 2011; 15(4): 413-426.
7. Salihu M, Ajayi BO, Adedara IA, et al. 6-gingerol-rich

- fraction from *Zingiber officinale* prevents hematoxicity and oxidative damage in kidney and liver of rats exposed to carbendazim. *J Diet Suppl* 2016; 13(4): 433-448.
8. Hashem MA, Mohamed WAM, Attia ESM. Assessment of protective potential of *Nigella sativa* oil against carbendazim- and/or mancozeb-induced hematoxicity, hepatotoxicity, and genotoxicity. *Environ Sci Pollut Res Int* 2018; 25(2): 1270-1282.
  9. Owumi SE, Nwozo SO, Najophe ES. Quercetin abates induction of hepatic and renal oxidative damage, inflammation, and apoptosis in carbendazim-treated rats. *Tox Res Appl* 2019; 3. doi: 10.1177/2397847319849521.
  10. Ertik O, Bayrak BB, Sener G, et al. Melatonin improves liver and pancreatic tissue injuries in diabetic rats: role on antioxidant enzymes. *J Diabetes Metab Disord* 2023; 22(1): 591-602.
  11. Shen S, Liao Q, Wong YK, et al. The role of melatonin in the treatment of type 2 diabetes mellitus and Alzheimer's disease. *Int J Biol Sci* 2022; 18(3): 983-994.
  12. Hyun M, Kim H, Kim J, et al. Melatonin protects against cadmium-induced oxidative stress via mitochondrial STAT3 signaling in human prostate stromal cells. *Commun Biol* 2023; 6(1): 157. doi: 10.1038/s42003-023-04533-7.
  13. Almeida LL, Pitombeira GSGN, Teixeira AAC, et al. Protective effect of melatonin against herbicides-induced hepatotoxicity in rats. *Toxicol Res (Camb)* 2021; 10(1): 1-10
  14. Akbulut S, Elbe H, Eris C, et al. Effects of antioxidant agents against cyclosporine-induced hepatotoxicity. *J Surg Res* 2015; 193(2): 658-666.
  15. Barangi S, Mehri S, Moosavi Z, et al. Melatonin inhibits benzo(a)pyrene-induced apoptosis through activation of the Mir-34a/Sirt1/autophagy pathway in mouse liver. *Ecotoxicol Environ Saf* 2020; 196: 110556. doi: 10.1016/j.ecoenv.2020.110556.
  16. Alghamdi SA. Effect of *Nigella sativa* and *Foeniculum vulgare* seeds extracts on male mice exposed to carbendazim. *Saudi J Biol Sci* 2020; 27(10): 2521-2530.
  17. Garcia MS, Cavalcante DNC, Araújo Santiago MDS, et al. Reproductive toxicity in male juvenile rats: antagonistic effects between isolated agrochemicals and in binary or ternary combinations. *Ecotoxicol Environ Saf* 2021; 209: 111766. doi: 10.1016/j.ecoenv.2020.111766.
  18. Balarastaghi S, Barangi S, Hosseinzadeh H, et al. Melatonin improves arsenic-induced hypertension through the inactivation of the Sirt1/autophagy pathway in rat. *Biomed Pharmacother* 2022; 151: 113135. doi: 10.1016/j.biopha.2022.113135.
  19. Marcon L, Bazzoli N, Honor Mounteer A, et al. Histological and histometric evaluation of the liver in *Astyanax bimaculatus* (Teleostei: Characidae), exposed to different concentrations of an organochlorine insecticide. *Anat Rec (Hoboken)* 2015; 298(10): 1754-1764.
  20. Yousef HN, Ibraheim SS, Ramadan RA, et al. The ameliorative role of eugenol against silver nanoparticles-induced hepatotoxicity in male Wistar rats. *Oxid Med Cell Longev* 2022; 2022: 3820848. doi: 10.1155/2022/3820848.
  21. Bradford MM. A rapid and sensitive method for the quantitation of microgram quantities of protein utilizing the principle of protein-dye binding. *Anal biochem* 1976; 72: 248-254.
  22. Ebedy YA, Elshazly MO, Hassan NH, et al. Novel insights into the potential mechanisms underlying carbendazim-induced hepatorenal toxicity in rats. *J Biochem Mol Toxicol* 2022; 36(8): e23079. doi: 10.1002/jbt.23079.
  23. Selmanoglu G, Barlas N, Songür S, et al. Carbendazim-induced haematological, biochemical and histopathological changes to the liver and kidney of male rats. *Hum Exp Toxicol* 2001; 20(12): 625-630.
  24. Mo E, Ebedy YA, Ibrahim MA, et al. Newly synthesized chitosan-nanoparticles attenuate carbendazim hepatorenal toxicity in rats via activation of Nrf2/HO1 signaling pathway. *Sci Rep* 2022; 12(1): 9986. doi: 10.1038/s41598-022-13960-1.
  25. Zhang L, Yuan X, Wang S, et al. The relationship between mitochondrial fusion/fission and apoptosis in the process of adipose-derived stromal cells differentiation into astrocytes. *Neurosci Lett* 2014; 575: 19-24.
  26. Yuan X, Zhang L, Wang S, et al. Mitochondrial apoptosis and autophagy in the process of adipose-derived stromal cell differentiation into astrocytes. *Cell Biol Int* 2016; 40(2): 156-165.
  27. Qian S, Wei Z, Yang W, et al. The role of BCL-2 family proteins in regulating apoptosis and cancer therapy. *Front Oncol* 2022; 12: 985363. doi: 10.3389/fonc.2022.985363.
  28. Miao Z, Miao Z, Teng X, et al. Melatonin alleviates lead-induced fatty liver in the common carps (*Cyprinus carpio*) via gut-liver axis. *Environ Pollut* 2023; 317: 120730. doi: 10.1016/j.envpol.2022.120730.
  29. Menendez-Pelaez A, Reiter RJ. Distribution of melatonin in mammalian tissues: the relative importance of nuclear versus cytosolic localization. *J Pineal Res* 1993; 15(2): 59-69.
  30. Ceraulo L, Ferrugia M, Tesoriere L, et al. Interactions of melatonin with membrane models: portioning of melatonin in AOT and lecithin reversed micelles. *J Pineal Res* 1999; 26(2): 108-112.
  31. Abdollahzade N, Majidinia M, Babri S. Melatonin: a pleiotropic hormone as a novel potent therapeutic candidate in arsenic toxicity. *Mol Biol Rep* 2021; 48(9): 6603-6618.
  32. Yang Z, He Y, Wang H, et al. Protective effect of

- melatonin against chronic cadmium-induced hepatotoxicity by suppressing oxidative stress, inflammation, and apoptosis in mice. *Ecotoxicol Environ Saf* 2021; 228: 112947. doi: 10.1016/j.ecoenv.2021.112947.
33. El-Sokkary GH, Nafady AA, Shabash EH. Melatonin administration ameliorates cadmium-induced oxidative stress and morphological changes in the liver of rat. *Ecotoxicol Environ Saf* 2010; 73(3): 456-463.
34. Zavodnik LB, Zavodnik IB, Lapshina EA, et al. Protective effects of melatonin against carbon tetrachloride hepatotoxicity in rats. *Cell Biochem Funct* 2005; 23(5): 353-359.
35. Zhang Y, Jia Y, Zheng R, et al. Plasma microRNA-122 as a biomarker for viral-, alcohol-, and chemical-related hepatic diseases. *Clin Chem* 2010; 56(12): 1830-1838.
36. Akbari G, Savari F, Mard SA, et al. Gallic acid protects the liver in rats against injuries induced by transient ischemia-reperfusion through regulating microRNAs expressions. *Iran J Basic Med Sci* 2019; 22(4): 439-444.